



Numerical Simulation of Local Reinforcement of Steel Column-Beam Connections

Badis, W.¹, Belkacem, M.² and Taleb, R.^{3*}

¹ Ph.D. Candidate, Department of Civil Engineering, University of Blida 1, Blida, Algeria.

² Professor, Department of Civil Engineering, Faculty of Technology, University of Blida 1, Algeria.

³ Associate Professor, Department of Civil Engineering, Faculty of Technology, University of Blida 1, Algeria.

© University of Tehran 2024

Received: 11 Jun. 2024;

Revised: 5 Aug. 2024;

Accepted: 26 Aug. 2024

ABSTRACT: This study examines the behavior of beam-to-column moment connections where the beam tension flange force is transferred to the column flanges through bolts attached to a welded end-plate or T-stub. A significant challenge with this type of connection is the potential inability of the column flange to develop the required design resistance, necessitating either an increase in size or local reinforcement. Three-dimensional finite element analysis models of nine T-stubs were developed using ABAQUS software to investigate the behavior of such connections when locally reinforced with non-welded stiffeners. The numerical simulation results were compared with available experimental data from the literature. The study evaluated the influence of different reinforcement types on the stress and displacement distribution at the column flange level. The effectiveness of using angles and channels as reinforcement was clearly demonstrated, with an observed improvement in connection strength of over 250% for models with channel plates and 280% for models with angle plates compared to the unreinforced model. Additionally, these reinforcements resulted in significantly lower displacement, with reductions of about 90% for both channel and angle plate models.

Keywords: Bolted Connection, End Plate T-Stub Connection, Reinforcement, Finite Element Model.

1. Introduction

The optimization of steel construction has become increasingly crucial as engineers face the challenge of managing significant forces at the connections of steel structural elements. Choosing appropriate materials and connection types is essential to achieve efficient and economical designs. This study focuses on bolted beam-column connections, the most common type, with

and without reinforcements (Wang et al., 2024a). Bolted connections, consisting of an end-plate welded to the beam end and fastened to the column flange by bolts, have been extensively researched since 1914 (Kaushik et al., 2013) to the present day (Shaheen, 2022; Herath et al., 2023; Yilmaz and Bekiroğlu, 2022; Nofaresti and Gerami, 2023; Luo et al., 2023; Wang et al., 2024b).

Various methods (analytical, experimental, and numerical simulations)

* Corresponding author E-mail: rafik.taleb@bregroup.com

have been employed to assess and enhance the performance of these connections (Krishnamurthy and Graddy, 1976; Bursi and Jaspart, 1998; Shi et al., 2007; Nip and Surtees, 2011; Prinz et al., 2014; Özkılıç, 2023; Meng et al., 2023). End-plate beam-to-column connections are used in steel structures for their performance and resistance to external moments and shear forces (Abidelah et al., 2012; Bahaz et al., 2018). These connections are typically considered semi-rigid, with their attractiveness primarily due to the simplicity and economy of their design and fabrication (Tartaglia et al., 2020; Özkılıç, 2021; Khani et al., 2024). To meet strength and stiffness requirements, local deformations need to be minimized.

Yielding of the column flange in the tension region (Abdollahzadeh and Ghobadi, 2014; Lyu et al., 2023), particularly in connections with a thin column flange, significantly affects the overall behavior. To mitigate this, two methods are commonly used: employing a column with a thicker flange or a horizontal stiffener. However, thicker flanges are often uneconomical as the extra thickness is only necessary at the connection region, and welding horizontal stiffeners can be costly. Researchers have explored the stiffening requirements of bolted connections on the tension side (Sherbourne, 1961; Zoetemeijer, 1974) and proposed various methods for stiffening the column flange opposite the beam tension flange. Sherbourne (1961) demonstrated through testing that the absence of stiffening in the tension zone significantly reduces both strength and stiffness.

Zoetemeijer (1974) found that backing plates considerably increased connection stiffness and strength, offering an alternative to traditional horizontal stiffeners. Packer and Morris (1977) performed a series of tests on T-stubs connected to columns representing the tension zone. Among the tested specimens, one was stiffened with 1/3 depth triangular stiffeners and another with full depth

stiffeners welded only to the column flange. They concluded that full-depth stiffeners were more effective than 1/3 depth triangular stiffeners. Moore and Sims (1986) investigated the influence of backing plates on extended end-plate connections by testing a number of T-stubs with backing plates of different lengths. They showed that backing plates effectively increase the yield load of extended end-plate connections.

T-stub tests carried out by Grogan and Surtees (1999) also showed that bolted backing angles significantly enhanced the performance of extended end-plate connections compared to traditional welded stiffeners. Tagawa and Gurel (2005) introduced a new stiffening method using bolted channels, which was effective in significantly increasing the yield load of bolted moment connections. Al-Khatib and Bouchair (2007) used finite element modelling to show the beneficial contribution of backing plates to strength and stiffness.

Sethi and Warda (2014) investigated the effect of using threaded bars on extended end-plate connections by testing a series of T-stubs to column connections. They concluded that backing plates effectively increased the yield load of extended end-plate connections. Strength improvement was observed when using both threaded bars and welded plates, with a more significant enhancement compared to using welded plates alone. A similar improvement was noted when combining threaded bars with backing plates. However, applying both threaded bars and channels did not provide any additional benefit in overall connection behavior compared to models reinforced with either threaded bars or channel plates individually.

Tagawa and Liu (2014) investigated bolted beam-to-column connections stiffened with steel member assemblies and confirmed that the proposed method using steel member assemblies is effective to stiffen the bolted end-plate connections.

Testing of one-side bolted T-stub through thread holes under tension strengthened with a backing plate, conducted by Zhu et al. (2017), showed that backing plates efficiently improve the tension strength. Boudia et al. (2020) analysed the mechanical behavior of bolted joints with extended end-plates and various stiffeners, noting the quantifiable stiffness and strength provided by end-plate stiffening.

Recently, the behavior of beam-to-column joints with and without stiffeners was investigated, focusing on the influence of geometrical characteristics on joint resistance, stiffness, and material cost optimization (Gašić et al., 2021). Despite the simplicity in the use of end-plate connections, their analysis remains complex due to multiple components affecting their behaviour.

Limited research studies have been conducted to assess the stress and displacement performance of bolted connections by stiffening the column flanges and webs, using backing angles and channels. The deformability of this connection type is largely governed by the deformation capacity of the column flange or end-plate and bolt elongation in the tension zone. While testing full-scale connections is the most accurate analysis method, it is often impractical due to high costs and complexity. Additionally, full-scale tests may struggle to pinpoint the causes of structural failures, even with extensive strain-gauging instrumentation. Therefore, the finite element method presents a viable alternative as it is well-suited for parametric analyses, allowing for the identification of the influence of various design parameters on the connection performance (Shabanzadeh et al., 2019).

This study selected nine T-stub column connections, representing the tension zone of an extended end-plate connection, based on Sethi's (1989) experimental work aimed to assess different types of column reinforcement schemes and propose a new reinforcement type that ensures ease of fabrication, cost-effectiveness, and

improved performance. Numerical simulations using ABAQUS software were conducted to validate and compare the results with experimental data. ABAQUS offers features like node contact elements, surface contact elements, and material nonlinearity that can be applicable to the problem of connection characterization (Sabuwala et al., 2005; Wang et al., 2020; Berrospi Aquino et al., 2021; Labibzadeh et al., 2025). The validated model was used to evaluate the mechanical performance of connections reinforced with various stiffener arrangements, focusing on displacements and stresses in the column flange.

This study aims to examine the effect of new alternative stiffeners (channel and angle plates) on the overall behavior of the connection using the finite element method. By supporting experimental results with additional numerical results that are difficult to obtain through testing, it was demonstrated that channel or angle plates are viable alternatives to traditional welded stiffeners or backing plates. These alternative stiffeners are important for reducing structural costs while maintaining high connection performance by increasing strength and reducing deformations.

2. Materials and Methods

2.1. Finite Element Analysis of the T-stub Connections

Finite element analysis was utilized to simulate nine T-stub connection models. Appropriate mesh and boundary conditions were applied to the T-stub connections, as detailed in next sections.

2.2. Geometric Details of Connections

This study considered nine tests on T-stub column connections, representing the tension zone of an extended end-plate connection (Kendall et al., 2024; Bao et al., 2019; Özkılıç and Topkaya, 2021) based on the experimental study carried out by Sethi (1989). All connections were fabricated from the same column section ($UC154 \times 154 \times 23$), and the same type of T-stub was

used (Figure 1). The reinforcement of the column flange increased progressively from test to test, as shown in Figure 2. All specimens in this series were connected

using M20 and M16 bolts grade 8.8. The thickness of the T-stub flange and web was kept constant at 24 mm across all tests.

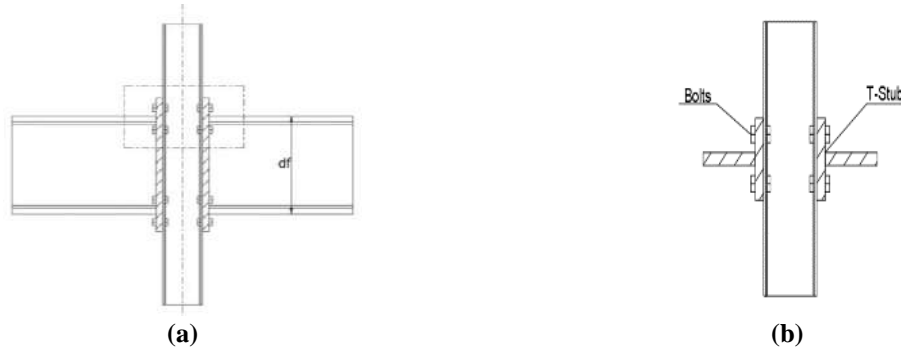


Fig. 1. a) Extended end-plate connection; and b) Its T-stub idealization

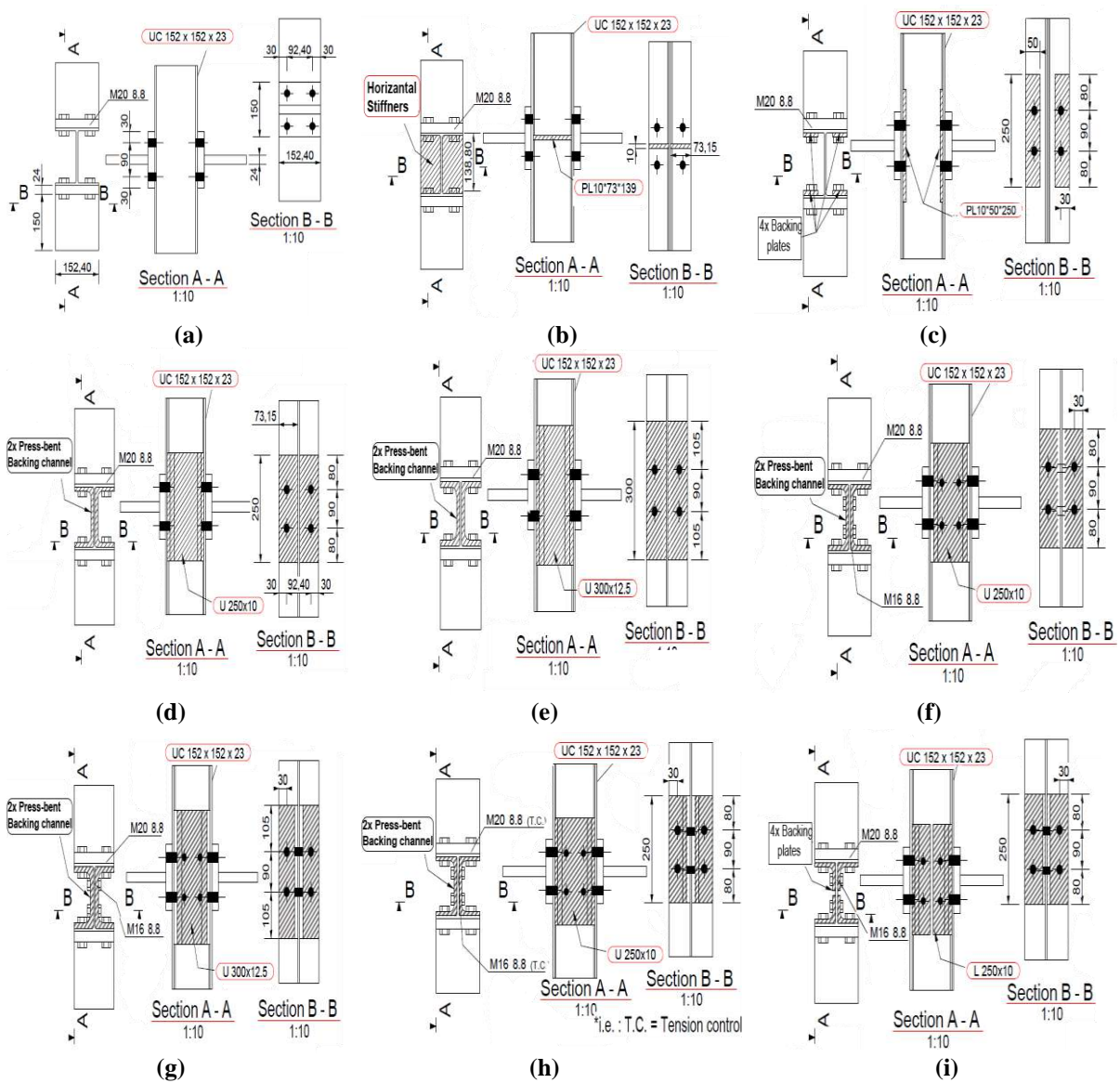


Fig. 2. Dimension and details of tests: a) T1 Test (un-reinforced); b) T2 Test (horizontal stiffeners); c) T3 Test (250 × 10 backing plates); d) T4 Test (250 × 10 backing channel); e) T5 Test (300 × 12.5 backing channel); f) T6 Test (250 × 10 backing channel bolted to col.web); g) T7 Test (300 × 12.5 backing channel bolted to col.web); h) T8 Test (250 × 10 backing channel bolted (HA bolts) to col.web); and i) T9 Test (250 × 10 backing angles bolted to col.web)

The size of the bolts and the dimensions of the T-stub flange, particularly its thickness, were intentionally chosen to be stronger than required to prevent bolt failure. This ensured that any failure would occur in the column flange.

2.3. Materials Properties

The material properties of the connection components, as shown in Table 1, were derived from test data. The elastic modulus and yield stress were determined through tensile tests on the web and flange of each column and beam, as well as the end-plate and stiffener (Sethi, 1989).

2.4. Finite Element Models

The general-purpose finite element analysis software ABAQUS (Abaqus,

2017) was used to develop an efficient and accurate three-dimensional numerical model of nine test specimens from Sethi (1989), as shown in Figure 3. The modeling process began with creating individual parts and then assembling these parts to form the connection. To simplify the model and reduce complexity, hexagonal bolt heads and nuts were represented as circular ones (Saravanan, 2009; Prabha et al., 2011), and washers were not modeled. The bolt holes were made 2 mm larger than the bolt size. Fillets in the angles were not modeled. Nonlinearity was incorporated into the numerical model through the material characteristics, which were defined by introducing the yield stress and plastic strain of each material.

Table 1. Material properties

Property	Column: UC154 × 154 × 23		T-stub		Stiffener plate
	Flange	Web	Flange	Web	
Tensile strength f_y (N/mm ²)	319	326	260	240	245
Elastic modulus E ($\times 10^3$ N/mm ²)	205	205	205	205	205

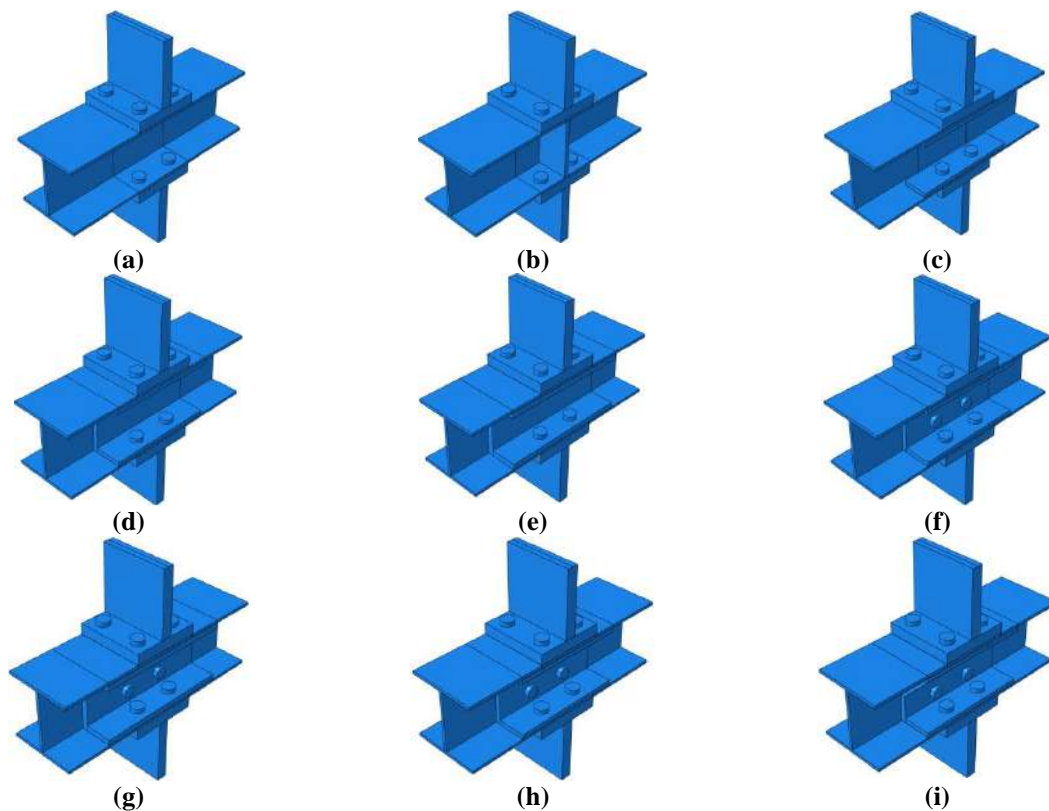


Fig. 3. 3D models for: a) M1 un-reinforced; b) M2 horizontal stiffener; c) M3 250 × 10 backing plates; d) M4 250 × 10 backing channels; e) M5 300 × 12.5 backing channels; f) M6 250 × 10 backing channels bolted to col.web; g) M7 300 × 12.5 backing channels bolted to col.web; h) M8 250 × 10 backing channels bolted (HA bolts) to col.web; and i) M9 250 × 10 backing angles bolted to col.web

Geometric nonlinearity was added by enabling the NLGEOM parameter in the STEP option of the ABAQUS program. The models also included contact and friction phenomena, as well as the pretension force in the bolts.

2.5. Element Type and Mesh Convergence

All parts of the connections were modeled using C3D8R elements, which are continuum three-dimensional 8-noded brick elements with reduced-order integration. This element has the ability to present large deformations and both geometric and material nonlinearities (Ghassemieh et al., 2021). Each node of this element has three degrees of freedom, corresponding to translations along the x, y, and z axes. First-order elements are generally more successful in reproducing yield lines and strain field discontinuities because some components of the displacement solution can be discontinuous at element edges. To mitigate the shear locking effect commonly associated with brick elements that use full integration (eight Gauss points) in bending simulations, a reduced integration element with one Gauss point is typically recommended (Selamet and Garlock, 2010).

2.6. Mesh Convergence

Since solid elements do not have a rotational degree of freedom (Lin et al., 2022), and to control hourglass mode problems in brick elements, the T-stub and

the column flange were discretized across the thickness (Nawar et al., 2021), as shown in Figure 4. Various mesh sizes were examined. The final finite element mesh arrangement was chosen based on processing time, solution convergence, and comparison with experimental results. Mesh sizes were controlled by the components of the connection to ensure proper surface-to-surface contacts and convergence (Lin et al., 2022).

2.7. Contact Modeling

A surface-to-surface contact approach was adopted for all contacts in the connection models. When defining a contact pair, two distinct surfaces are required, with no shared nodes, and a master and slave surface must be designated. The contact surfaces of the bolt shank, bolt head, and bolt nut were modeled as master surfaces due to the higher stiffness of the bolt material. In the contact between the column and T-stub, the column face was defined as the master surface because the column is made of higher-grade steel compared to the end-plates. Similarly, in the contact between the column and the stiffeners, the column face was designated as the master surface. The surfaces interfacing with the master surfaces were defined as slave surfaces. Frictional contact ($\mu = 0.3$) using penalty stiffness formulation was considered for the tangential contact between the T-stub and column flange (Figure 5a) and between the stiffeners and column flange (Figure 5b).

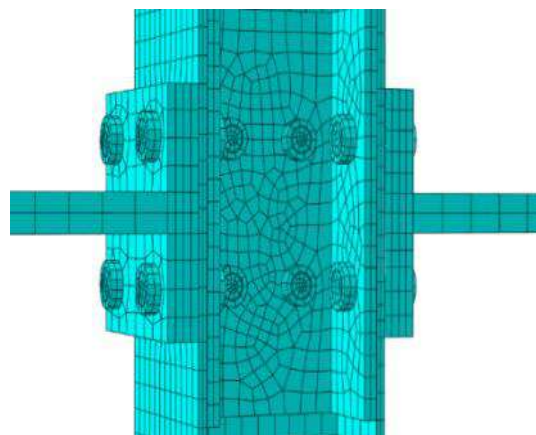


Fig. 4. Finite element mesh of the T-stub connections

To prevent penetration between elements in contact pairs, the normal contact was defined as hard using the augmented Lagrange formulation (Nawar et al., 2021). A hard constraint was applied to the connection of the bolt head/nut to the T-stub/column/stiffeners (Figure 5c). The tangential contact between the bolt hole and the bolt shank was considered frictionless to prevent penetration of the bolt into the connection plates (Figure 5d). The normal contact was also defined as hard, and small sliding of the surfaces was considered.

2.8. Load Application and Boundary Conditions

Loading was applied as a series of

concentrated forces at the outer edge of the T-stub web to simulate the effect of a uniformly distributed load. Both ends of the column were fully restrained. For most models, the load was applied in a single step. However, for the M8 model, the loading was applied in two steps (Figure 6). In the first step, pre-tensioning forces were applied to all the bolts, calculated using Eq. (1).

$$F_p = 0.7 \times A_s \times f_u \quad (1)$$

where A_s : is bolt nominal section, f_u : is bolt ultimate load ($f_u = 800$ MPa as the bolts are of grade 8.8). In the second step, a uniform pressure load was applied to the T-stub column.

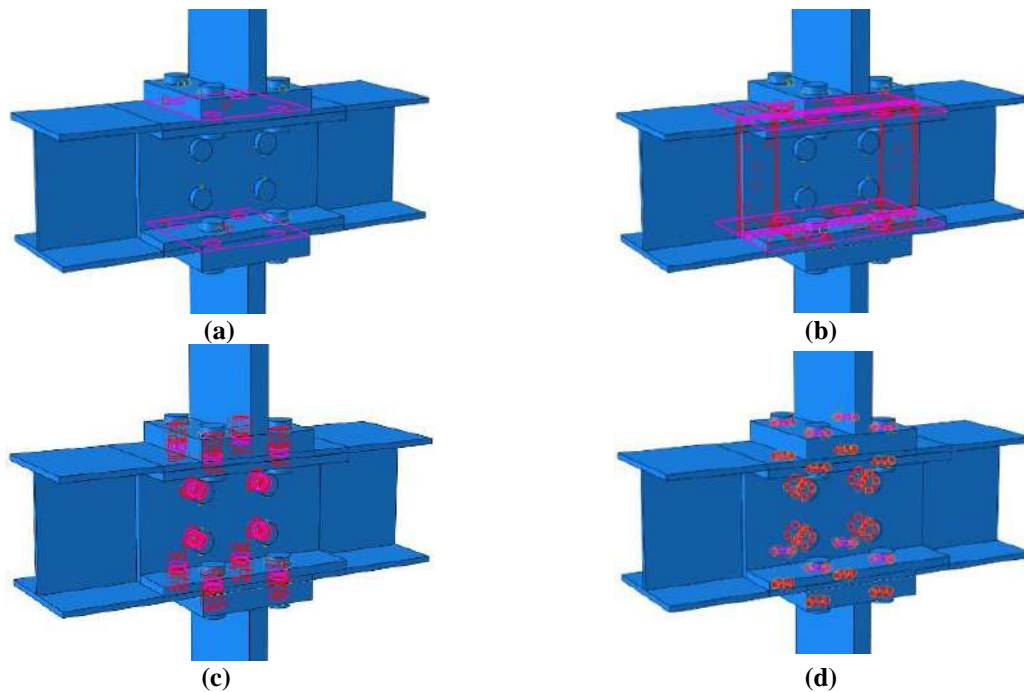


Fig. 5. Contact interactions and ties constraint of the models: a) Contact between the T-stub /column flange; b) Contact between the stiffener /column flange; c) Contact between the T-stub /column flange hole to the bolt shank; and d) Tie constraint bolt head/nut to the T-stub/column/stiffeners

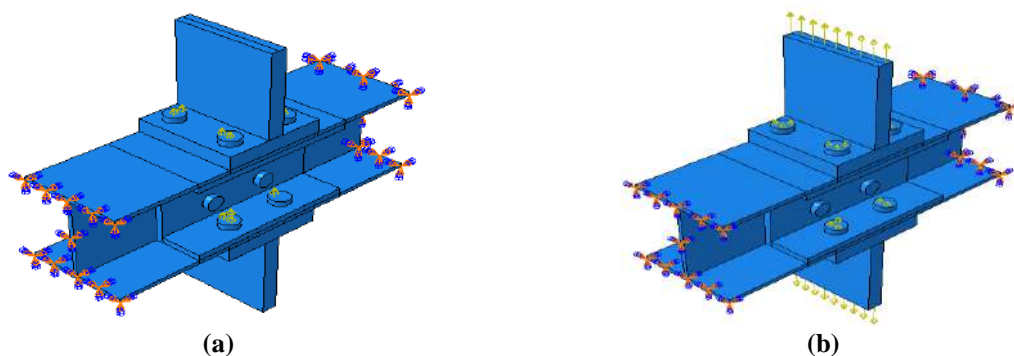


Fig. 6. Load application and boundary conditions: a) Step 1; and b) Step 2

Given the highly non-linear nature of the models, there is a potential risk of non-convergence in the solution. This issue is addressed by utilizing ABAQUS's non-linear analysis capabilities, which automatically selects appropriate load increments and convergence tolerances for non-linear analyses. It also continually adjusts these parameters throughout the analysis to ensure accurate and efficient results.

2.9. Validation of the Proposed Finite Element Models

Figure 7 shows comparisons between the load-displacement curves of the different numerical models and the available experimental tests. The load versus displacement results for M1 model and test T1

(unreinforced flange) are shown in Figure 7a, indicating that the experimentally measured values are in good agreement with the corresponding finite element results. Indeed, the two curves are almost identical, and the finite element analysis accurately predicts the experimental results.

This suggests that the modeling of the unreinforced tension region is satisfactory, the element used, and the contact between plates are also satisfactory. The same tendency is observed in the case of model M2 with the experimental test T2 (Figure 7b). For the model M3 with test T3, it can be seen that up to 100 kN, the two curves are similar, as illustrated in Figure 7c. This indicates that the model and the test behaved in the same manner and presented the same stiffness.

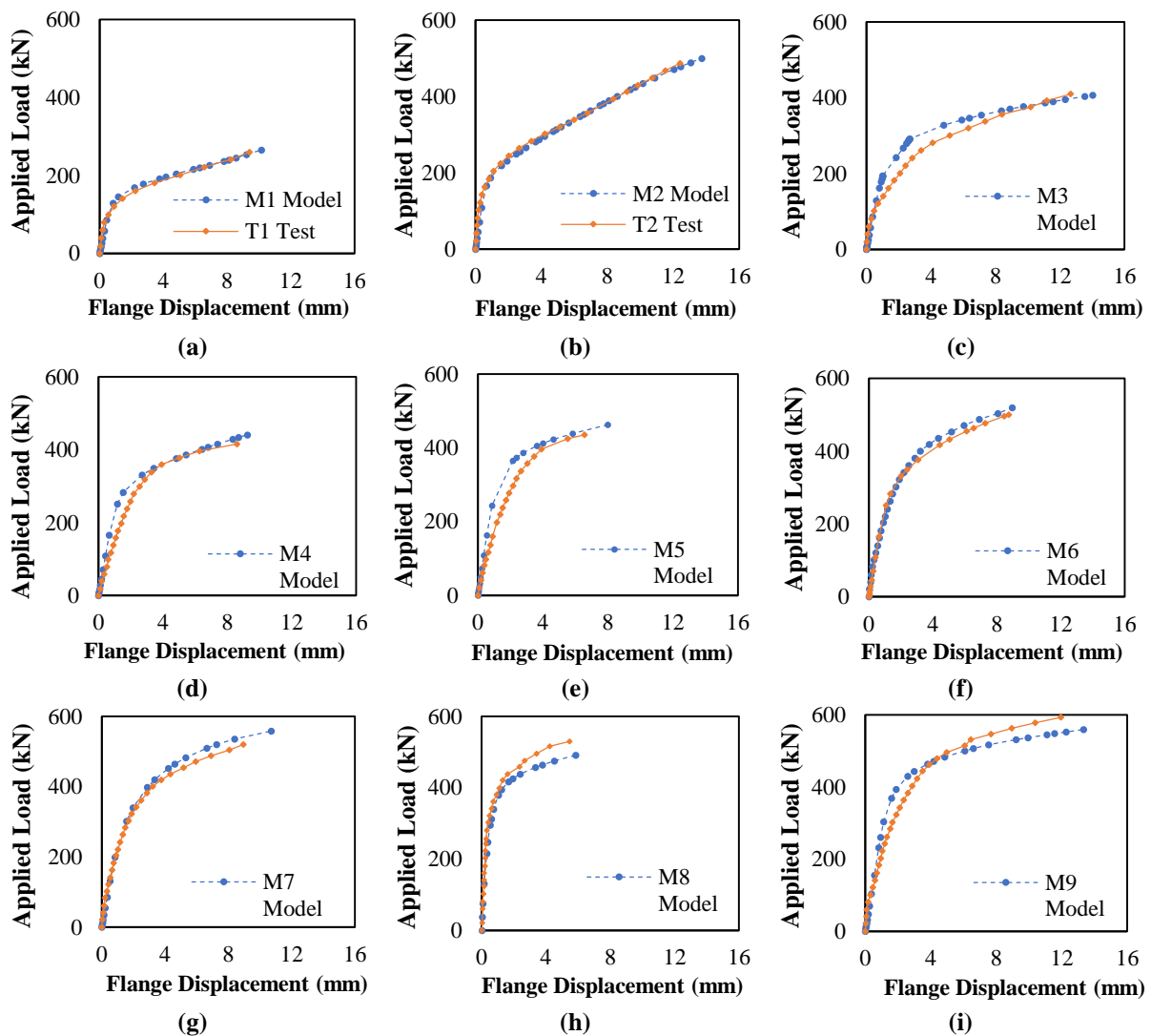


Fig. 7. Load-displacement curves of the numerical models and experimental tests: a) Comparison between M1 model and T1 test; b) Comparison between M2 model and T2 test; c) Comparison between M3 model and T3 test; d) Comparison between M4 model and T4 test; e) Comparison between M5 model and T5 test; f) Comparison between M6 model and T6 test; g) Comparison between M7 model and T7 test; h) Comparison between M8 model and T8 test; and i) Comparison between M9 model and T9 test

However, beyond 100 kN load, the predicted displacement from the finite element analysis is higher than the corresponding test results up to 375 kN. It can be noticed from Figure 7d that the model M4 is both stiffer and stronger than the test T4. The finite element result does not correlate well with the experimental results up to 350 kN. Beyond this load, the two curves are similar. The most likely reason for this is that the channel plates in model M4 seem to stiffen the column flange more than was the case with test T4. The same trend was observed for model M5 compared to test T5 (Figure 7e). The load versus deformation results for models M6 and M7 are illustrated in Figures 7f and 7g, respectively. The models and tests show similar behavior, with the finite element model results closely matching those of the tests.

Figure 7h shows the load-displacement curve for the model M8 compared to the load-deformation diagram for the test T8. The model accurately predicted the experimental result up to 400 kN. Beyond this load, the model shows less stiffness. It can be seen from that the model M9 is both stiffer and stronger than the test T9 up to approximately 450 kN, beyond that load, the test shows higher stiffness. Figure 8 summarizes the difference between numerical and experimental results in terms of yield load and corresponding displacement for the nine models. The highest difference of yield load is reached

in M1 and M3 models, this difference is estimated around 40% and 26.7%, respectively, and it decreases by 2.40% for the M6 model. Furthermore, the highest difference of displacement is reached in model M1 by 33.33%, and it decreases in the M5 model by 2.27% compared to experimental tests T1 and T5, respectively.

The simplifications introduced in the numerical models in order to reduce their complexity (Luo et al., 2020), the initial imperfection, the material modeling, the type of analysis, and the mesh sensitivity are the most common factors that can lead to the differences between the results obtained for numerical models and experimental tests.

3. Results and Discussion

3.1. Yield Load and Load Capacity

In order to compare the various model results (M4 to M9) and the results from unstiffened, horizontally stiffened, and backing plates stiffening models (M1, M2, and M3), the yield load and load capacity corresponding to a joint rotation of 30×10^{-3} rads were determined. This rotation value is the maximum rotation for a beam column connection suggested by Surtees and Mann (1970), a typical beam and column combination (UB 254 \times 102 \times 22 and UC 152 \times 152 \times 23) were assumed. A horizontal displacement ($D_m = 7.8$ mm) between the column flange and T-stub flange resulting from a rotation of $\alpha = 0.03$ rad was computed using Eq. (2).

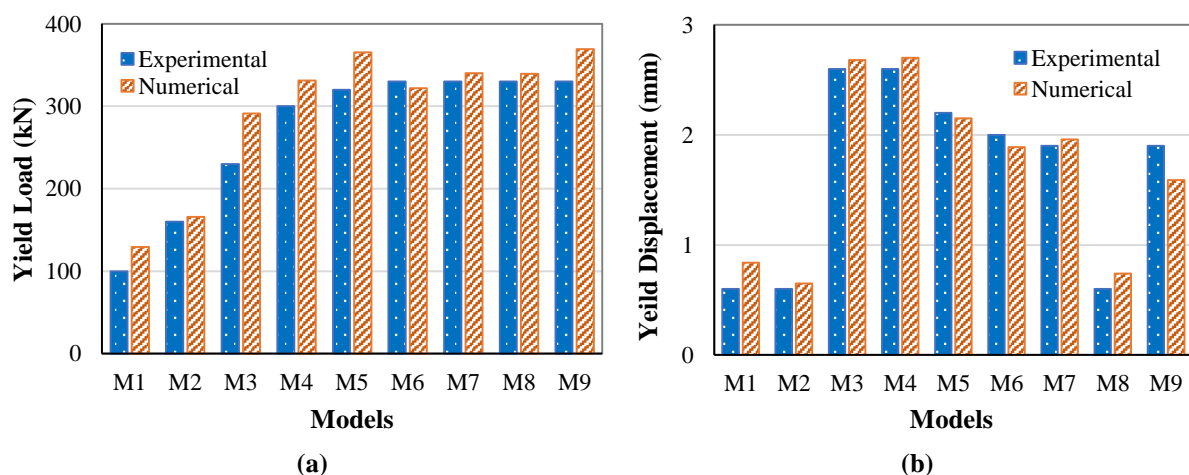


Fig. 8. Comparison between numerical and experimental results for: a) Yield load; and b) Yield displacement

The load corresponding to the displacement D_m was determined as Eq. (2).

$$D_m = d_f \times \tan \alpha \quad (2)$$

where d_f is the distance between the centers of beam flanges as shown in Figure 1.

Figures 9 and 10 summarize the yield and capacity loads obtained for the different analyzed models. Comparing the stiffened models with the unstiffened model M1, model M9 (250 × 10 mm backing angles bolted to the column web) has the highest strength and stiffness. It is the best model in terms of strength and stiffness. The yield load and the load capacity of model M9 are about 2.85 and 2.26 times, respectively, of those observed for model M1. A similar trend is observed for model M2 (horizontally stiffened), where the yield load and the load capacity are about 2.22

and 1.43 times, respectively, of that observed for model M1. As can be seen in Figures 9 and 10, the yield and load capacity are about 1.26 and 1.45 times in comparison to that of M1. Models M7 (300 × 12.5 mm backing channel bolted to column-web) and M8 (250 × 10 mm backing channel bolted (HA bolts) to column-web) share practically the same results, their yield load is about 2.6 times that observed in model M1, and the load capacity is about 2.2. Hence, it can be concluded that increasing the thickness and length of the channel plate or pre-tensioning the bolts have the same effect on strength and stiffness. Comparing between models M5 and M7 that use the same stiffener (300 × 12.5 mm backing channel), model M5 carried a higher yield load but less load capacity.

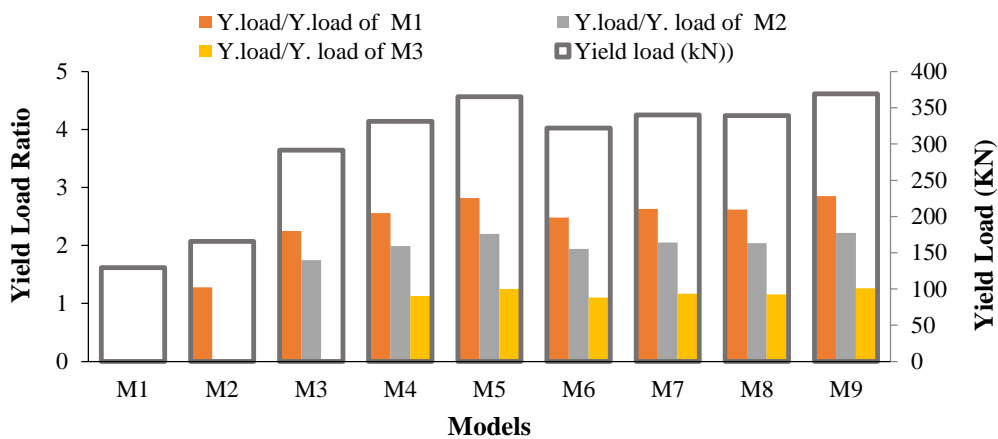


Fig. 9. Comparison of yield load between the nine models

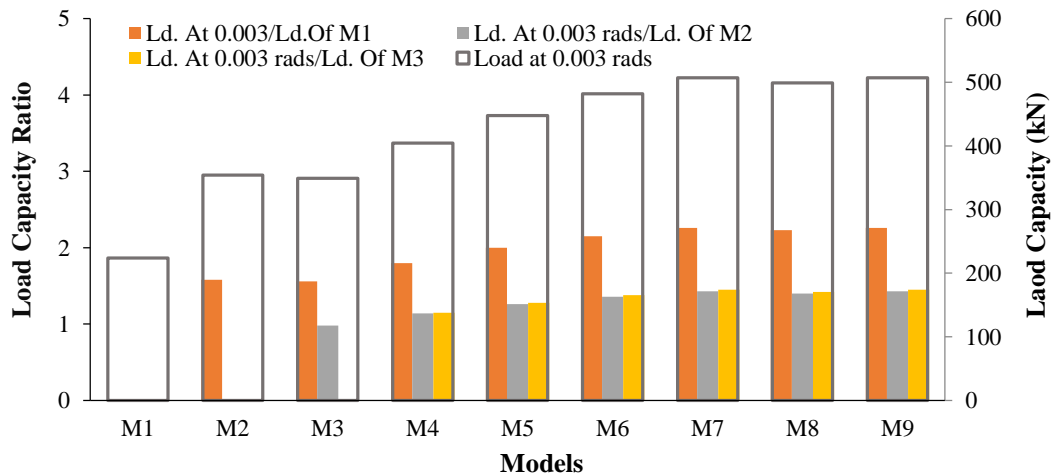


Fig. 10. Comparison of load capacity at 0.003 rads between the nine models

Therefore, using bolts to attach a channel plate to a column web has no effect on the yield load improvement. From the numerical results obtained for the nine models, it can be concluded that the method of stiffening the column flange with channels and angle plates is far more effective than using a horizontal stiffener or backing plates. Both strength and stiffness

are increased significantly.

3.2. Column Flanges and Web Stress and Displacement

Figures 11 and 12 illustrate the column flange and web stress and displacement of the nine numerical models analyzed, respectively.

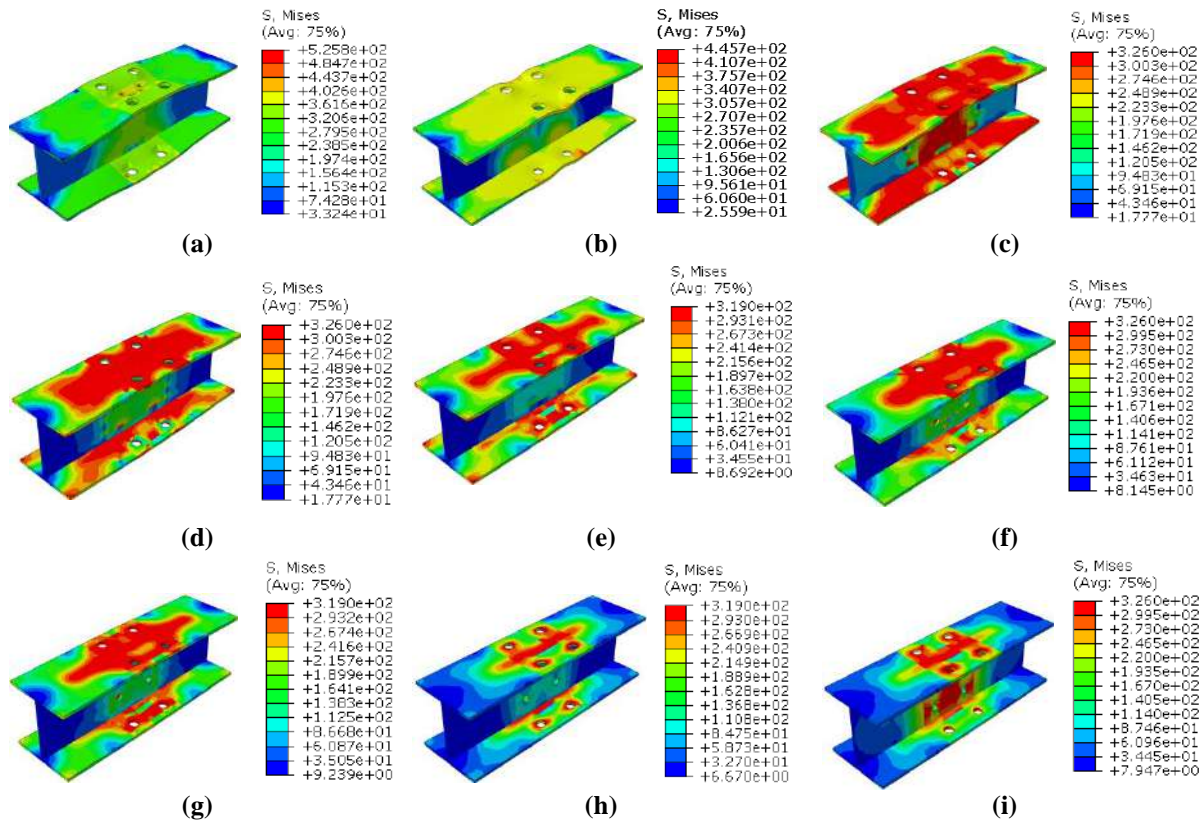
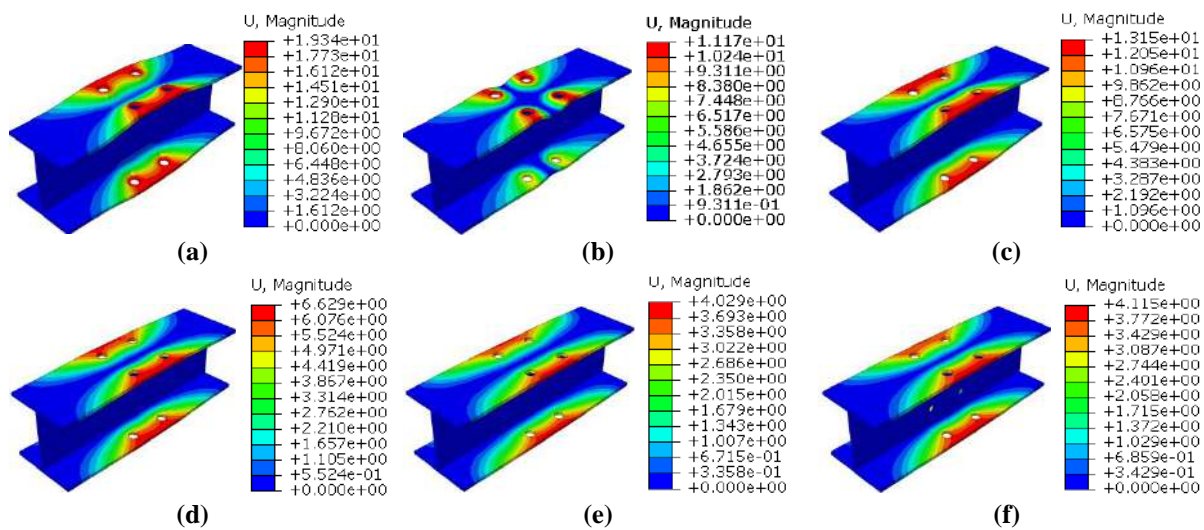


Fig. 11. Column flange stress of the numerical models: a) M1; b) M2; c) M3; d) M4; e) M5; f) M6; g) M7; h) M8; and i) M9



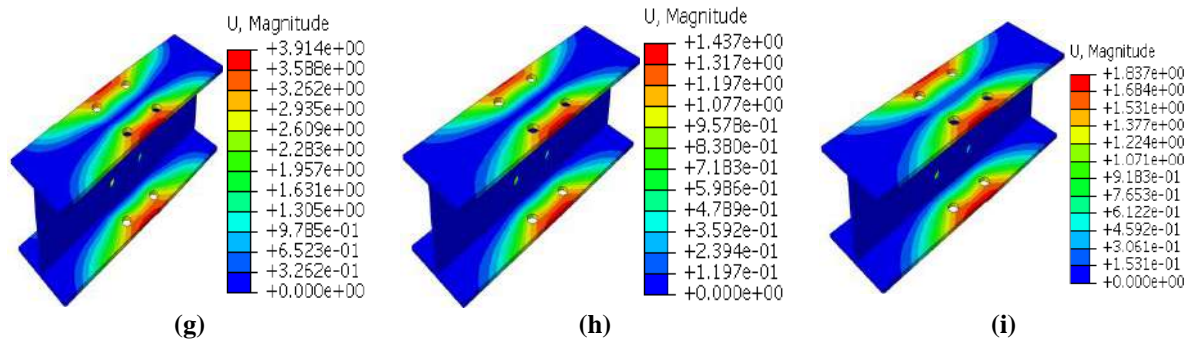


Fig. 12. Column flange displacement of the numerical models: a) M1; b) M2; c) M3; d) M4; e) M5; f) M6; g) M7; h) M8; and i) M9

Figure 11a clearly indicates that the flanges and the web of the column in the numerical model M1 were highly stressed by the loading. It represents the maximum stresses in the column flanges among the studied models. The unreinforced model (M1), as shown in Figure 13, also gives the largest displacement value (19.35 mm). This justifies the need of adding stiffeners. It can also be noticed that the high stresses affect almost all the flanges as well as a considerable part of the column web.

For the reinforced model (M2) with a 10 mm thick horizontal stiffener (Figure 12b), a significant decrease of the displacement in the middle-flange is noticed compared to model control M1 (Figure 13). This could be due to the presence of the horizontal stiffener. In terms of flange stresses, smaller values were found as compared to model M1. It is also noticed that the area of the flanges subjected to stresses is smaller than that of model M1 (Figure 11b). The stiffener plays an important role in this distribution, since this stiffener takes up a good part of the stresses.

The horizontal stiffener in the M2 model does not appear to affect the stress value at the web (Figure 13b). The horizontal stiffener only adds a local and punctual improvement. The M3 model, which is reinforced with backing plates at each flange (Figure 13a), shows the highest displacement at the flanges of the column in comparison with the unreinforced model (M1) and the other models. However, the stress of the flanges remains close to the M2 model (Figure 11). In contrast, the

displacements have dropped by 32% compared to the M1 model. The backing plates do not prevent excessive deformation.

Adding the backing plates to the flanges does not make them rigid. The stress of the web is the same as M1 and M2 models (Figure 13b). The results of the M4 model shows a significant decrease in the displacements of the flanges by 65.72% compared to the unreinforced model (M1). The web of the column does not seem to be very stressed (Figure 11d). The contribution of the U-shaped reinforcement seems to relieve the web of the column. The lowest stress values at the web are given by the model M5 as can be seen in Figure 13b.

It can be argued that the U-shaped reinforcement (without the bolts with the web) seems to relieve the web of the column. The same behavior is observed for the model M6, since it contains the same channel U with greater thickness and length. However, the presence of the bolts in the web increases the web stresses of the column. There is a drag effect from the bolts, which explains the small percentage of reduction compared to the M5 model. However, these reinforcements in the M5 and M7 models did not bring any change in the stresses in the flanges compared to the other models. In terms of displacement, the two models gave a much lower displacement of 79%. The dimensions of the reinforcement have a significant effect on the behavior of the T-stub connection.

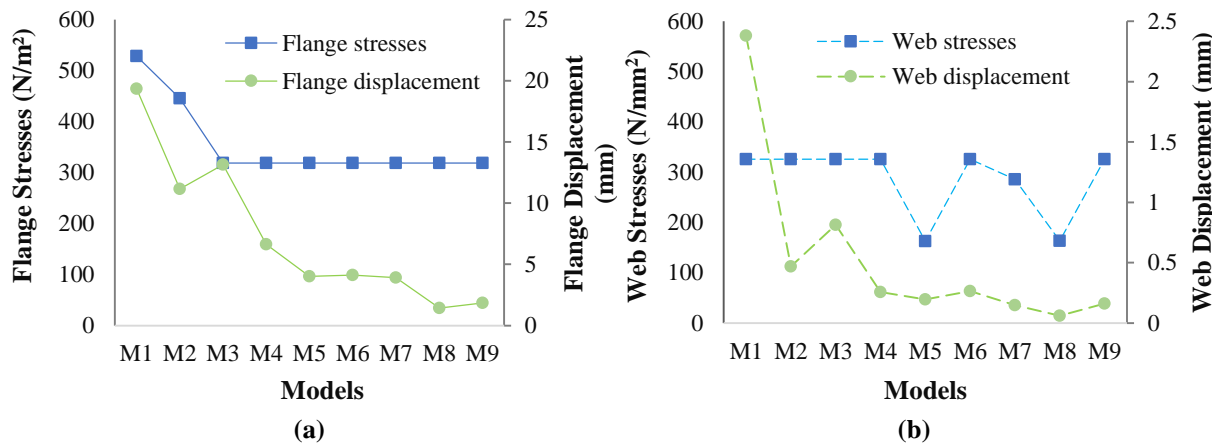


Fig. 13. Stresses and displacement at: a) Column flange; and b) Column web of the numerical models

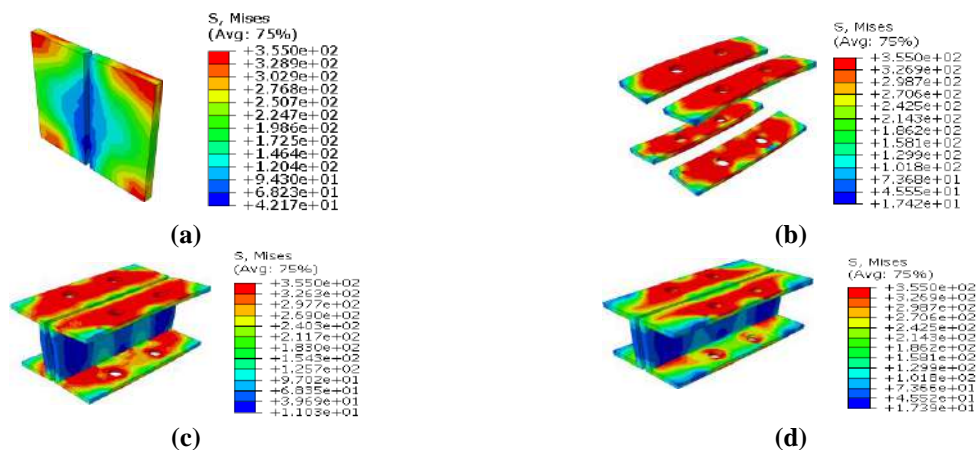
In the case of the reinforcement, backing Channel bolted to column’s web and flange (M6), a reduction of 78.75% in the displacement of the flange is noticed (Figure 13a). The presence of the bolts connecting the U-shaped reinforcement of the M6 model with the web improvement in the stresses compared to the M4 model. The presence of the U-shaped reinforcement relieves the web by taking a large part of the stresses, and therefore adding the bolt does not have significant effect.

The reinforcements in models M8 and M9 gave the lowest displacement. Thus, a reduction of 92.57% was found in model M8 and a reduction of 90.50% in model M9. The M8 and M9 models appear to have higher stiffness than the other models. Pre-tensioned bolts reduce displacement and increase stiffness (Model M8). It is noted that the preloaded bolts make the reinforcement more effective for the web. However, the reinforcement angles of the

M9 model did not improve the stresses in the web, which can be explained by the non-continuity of the angles in the web.

3.3. Stiffeners Stress and Displacement

Figures 14 and 15 illustrate the stiffeners von Mises stresses and displacement of the eight numerical models analyzed, respectively. Figure 15 shows the stiffeners displacement of the T-stub connection for the FE models. It can be seen from this figure that the higher displacement of the stiffener is observed for the T-stub connection reinforced by the backing plates (M3 model). In this model, the backing plates are not linked and seems to be entrained by the column flanges. For this reason, the deformation reaches a peak value of 13.40 mm. The lower displacement value is given by the M2 model. This could be attributed to the stiffness of the column web with the stiffener, which forms a unified body.



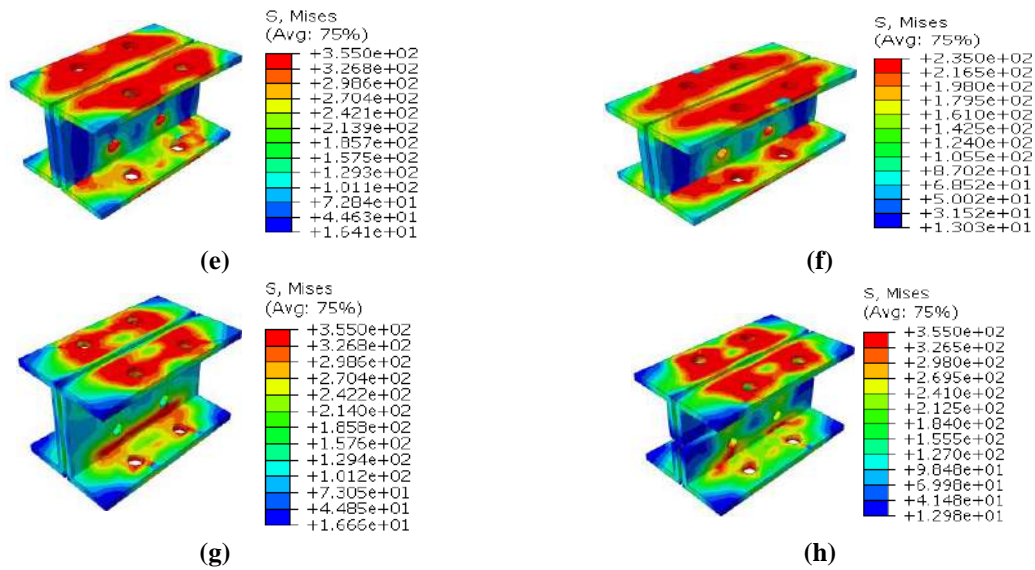


Fig. 14. Von Mises stresses of the stiffeners: a) M2; b) M3; c) M4; d) M5; e) M6; f) M7; g) M8; and h) M9

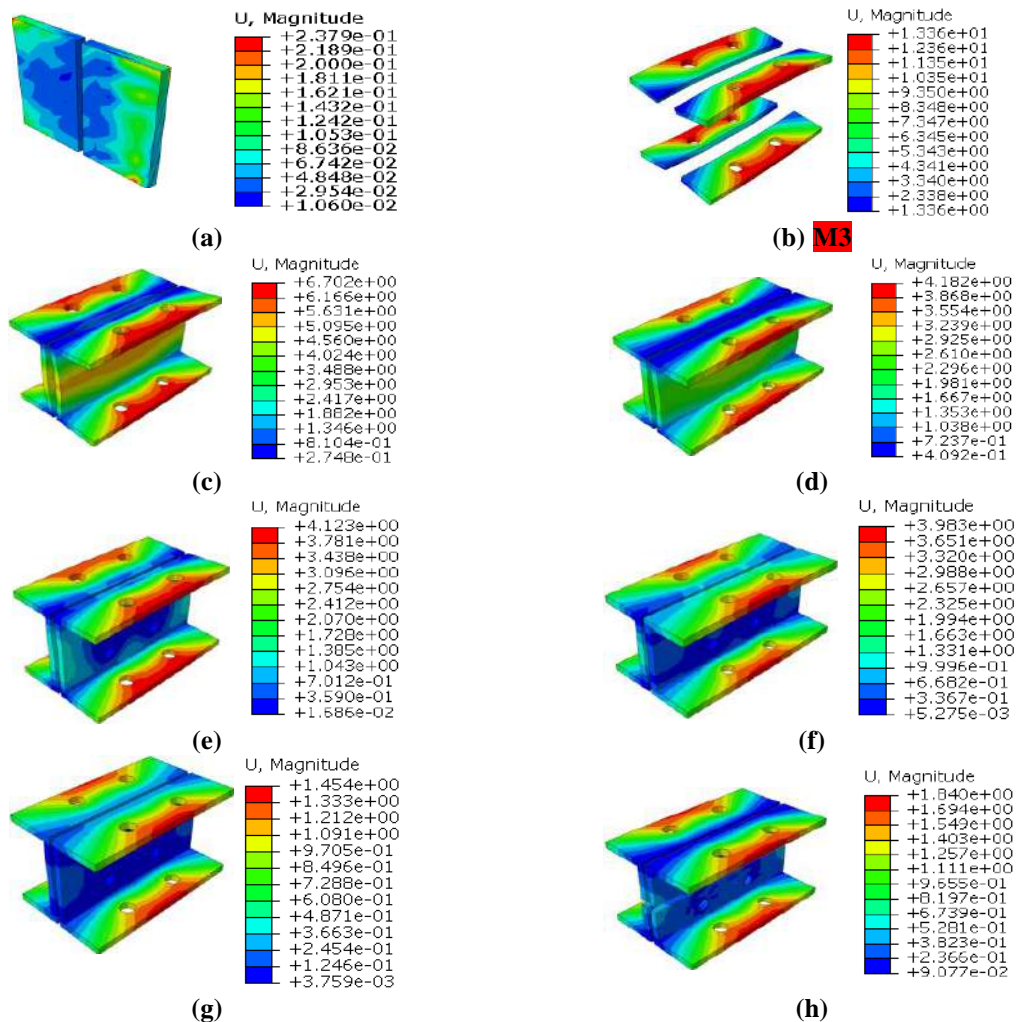


Fig. 15. Stiffeners displacement: a) M2; b) M3; c) M4; d) M5; e) M6; f) M7; g) M8; and h) M9

In the case of the M4 and M5 models, the displacements were 4.18 mm and 6.70 mm, respectively. The higher thickness (12.5 mm) and the length of the

reinforcement of the M5 model explain this low value. It should be noted that the M6, M7, M8, and M9 reinforcements have four bolts connecting them to the column web.

The M6 and M7 models give a maximum displacement of 4.12 mm and 3.98 mm, respectively. This may be attributed to the higher length and thickness of the M7 compared to the M6 model.

Comparing the stiffener displacement of the different analyzed models shows that M8 and M9 models give the lowest displacement values. The reinforcement of model M8 seems to have a higher stiffness compared to M9. This is due to the type of stiffener (two angles) used in the latter model. It should be remembered that in the M7 model, the reinforcement is of U-type with a thickness of 12.5 mm, as in the M5 model, but the latter gives a different behavior because of the absence of bolts connecting the reinforcement with the web of the column.

It should be noted that the presence of pre-stressed bolts in the M8 model does not improve the work of the reinforcements compared to the stresses in the M6 model reinforcement, which is equipped with normal bolts in the web of the column. It is clearly shown in Figure 16 that the addition of stiffeners played an important role in the overall performance, especially the stiffeners used in models M8 and M9, and this is what both researchers Grogan and Surtees (1999) and Tagawa and Gurel (2005) indicated in their research. Through

their study, they showed that channels and angle plates stiffeners have a clear effect in improving both strength and deformation compared to traditional stiffeners, and this is what we also confirmed through our study.

3.4. Bolts Stress and Displacement

Figures 17 and 18 show the bolts stresses and displacement, respectively. Figure 18 shows the bolts displacement of the T-stub connection for the FE models. It can be seen from this figure that the higher displacement of the bolts is observed for the M1 model, and the lowest value is observed for models M9 and M8, respectively. M1 model also represents the highest stress while M2 model represents the lowest one (Figure 17). As can be seen from Figure 19, the higher reduction in bolt stresses is noticed for M2 and M9 models. The bolts that work the least are those of the M9 model and represents a significant drop of 91.30% in bolt displacement compared to the M1 model. In the case of the M3 model, a reduction of 54% and 30.90% in bolt stresses and in bolt displacement, respectively, was noticed compared to the M1 model. The displacement reduction is the smallest compared to the other models, which means that the addition of the backing plates provides less stiffness compared to the other stiffener shapes.

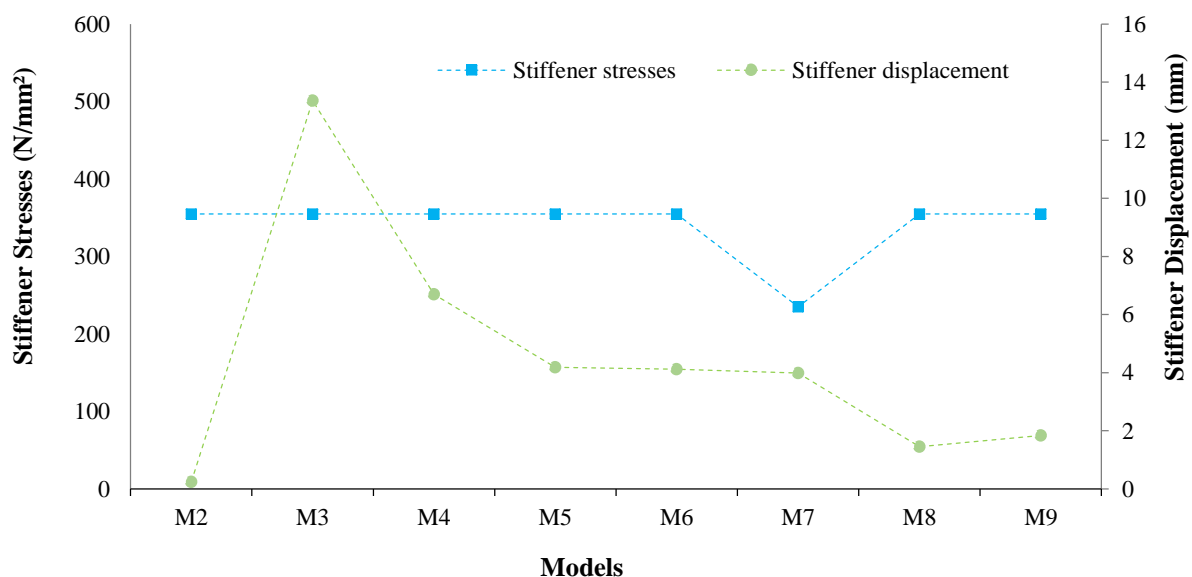


Fig. 16. Stiffener stresses and displacement of the numerical models

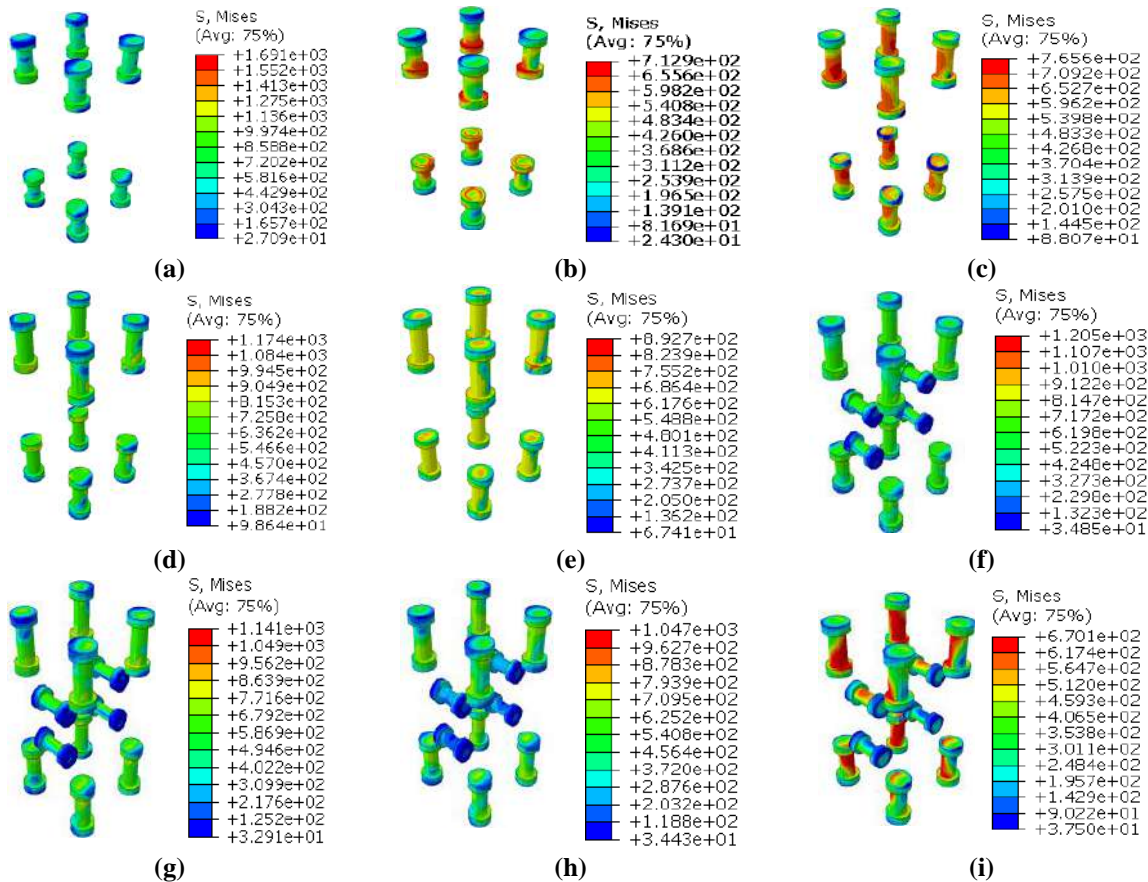


Fig. 17. Bolts stresses: a) M1; b) M2; c) M3; d) M4; e) M5; f) M6; g) M7; h) M8; and i) M9

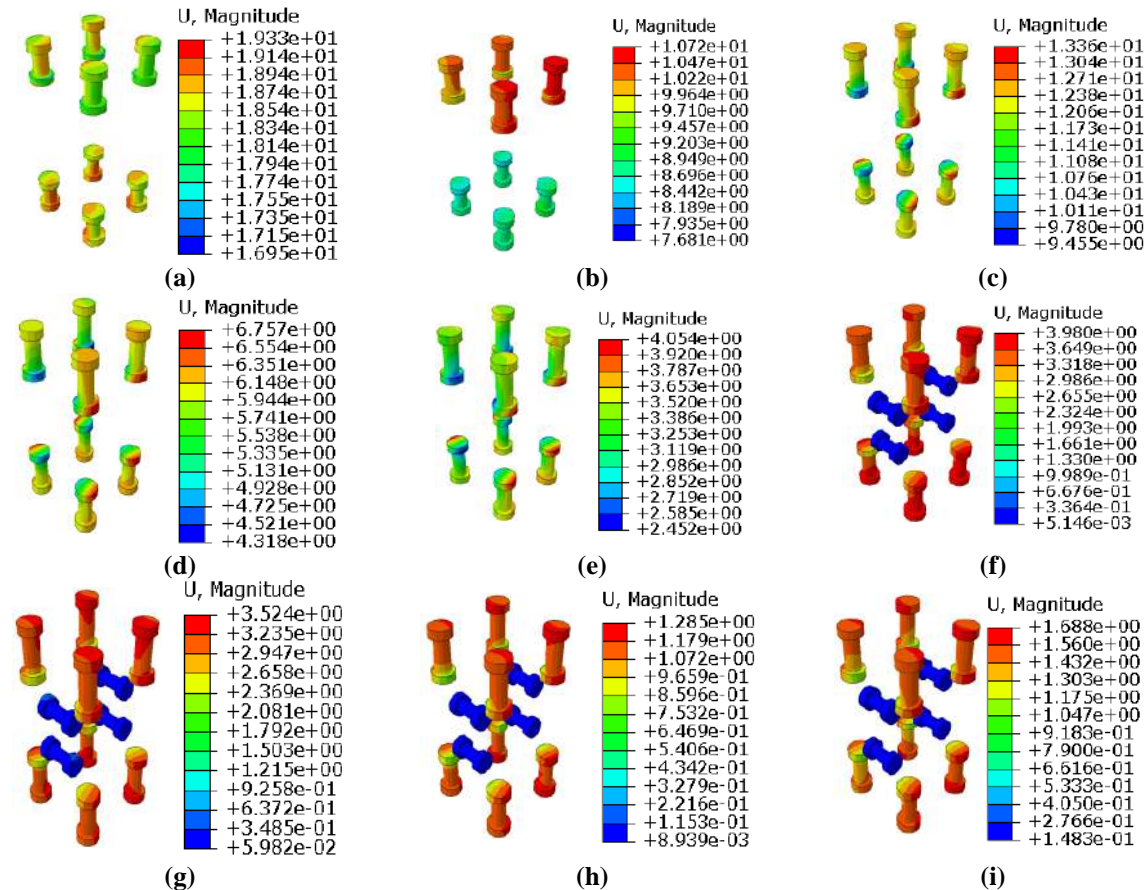


Fig. 18. Bolts displacement: a) M1; b) M2; c) M3; d) M4; e) M5; f) M6; g) M7; h) M8; and i) M9

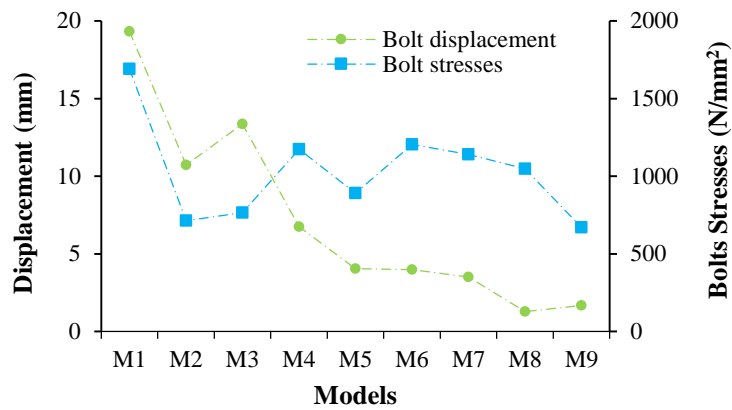


Fig. 19. Bolts stresses and displacement for M1 to M9 models

Models M4 and M6 give a low reduction of the bolt displacement compared to the M1 model. The bolt stresses are high. The U-shaped reinforcement with or without the absence of bolts in the web puts a lot of stress on the bolts. This can be explained by the lack of high-strength bolts in the web. This conclusion can be confirmed by the results obtained for the bolt displacement, where it can be seen that M4 and M6 models show a smaller reduction compared to the M8 model, which is bolted to the column web with preloaded bolts.

The M5 and M7 models with 12.5 mm thick U-shaped reinforcements give a stress reduction of 32% and 47% for the M7 and M5 models, respectively. The presence of the bolts with the web in the M7 model makes the assembly rigid and prevents the bolts from moving to allow part of the forces to be converted into deformation energy. Thus, the stresses in the bolts are very high. Both models represent practically the same displacement reduction, which was in a range of 20%.

The preloaded bolts in the M8 model result in lower column stresses and bolt forces than the M6 model with non-preloaded bolts. The M8 model represents the largest reduction in bolt displacement of 93.35% while the M6 model shows a reduction of 79.40%. This is due to the existence of pre-loaded bolts at the web of the column. All these stresses are particularly concentrated at the contact surfaces of the bolts with the flanges.

Models M1 and M9 give the extreme stress values (the lowest for M9 and the highest for M1), the stress drops by 60%.

4. Conclusions

This research investigated bolted T-stub to column connections under applied loading perpendicular to the column flange, initially without reinforcement. The numerical results were validated by comparing them to existing experimental data. A parametric study of eight geometric configurations was subsequently conducted to assess the impact and contribution of various components (stiffeners and bolts) on the connections' mechanical performance. The main conclusions are as follows:

- A finite element model was developed using ABAQUS software. The C3D8R element type used in the modeling proved to be suitable for nonlinear analysis of the T-stub to column connections.

- The load-displacement curves obtained by the numerical simulations showed a similar trend compared to the experimental curves, indicating that the numerical models are reliable for parametric studies.

- The most effective reinforcement method for the column flange in the tension region was found to be using backing channels, which resulted in a more than 250% improvement in strength compared to the unreinforced model. Angled plates bolted to the column flange also provided significant reinforcement, achieving a

280% increase in strength.

- Among the reinforcement options, backing channels and angled plates (M8 and M9 models, respectively) were identified as the most effective stiffeners.

These stiffeners enhance the column's ability to resist forces while maintaining acceptable deformation levels. The introduction of reinforcements led to a notable improvement in the connection behavior, positively affecting both the flanges and the web of the column compared to the non-reinforced configuration.

5. Declaration

During the preparation of this work, the authors solely used artificial intelligence (AI)-assisted tools to check grammar, spelling, grammar, readability, and sentence structure in certain sections of the manuscript. All content was critically reviewed and verified by the authors, who take full responsibility for the final manuscript.

6. References

- ABAQUS, I. (2017). "Abaqus user's and theory manuals (Version 6.17)", *Dassault Systemes Simulia Corp Providence, RI, USA*.
- Abdollahzadeh, G.R. and Ghobadi, F. (2014). "Mathematical modeling of column-base connections under monotonic loading", *Civil Engineering Infrastructures Journal*, 47(2), 255-272, <https://doi.org/10.7508/cej.2014.02.008>.
- Abdelah, A., Bouchair, A. and Kerdal, D.E. (2012). "Experimental and analytical behavior of bolted end-plate connections with or without stiffeners", *Journal of Constructional Steel Research*, 76, 13-27, <https://doi.org/10.1016/j.jcsr.2012.04.004>.
- Al-Khatib, Z. and Bouchair, A. (2007). "Analysis of a bolted t-stub strengthened by backing-plates with regard to Eurocode 3", *Journal of Constructional Steel Research*, 63(12), 1603-1615, <https://doi.org/10.1016/j.jcsr.2007.01.012>.
- Bahaz, A., Amara, S., Jaspert, J.P. and Demonceau, J.F. (2018). "Analysis of the behaviour of semi rigid steel end plate connections", In: *MATEC Web of Conferences*, 149, 02058, <https://doi.org/10.1051/mateconf/201814902058>.
- Bao, W., Jiang, J., Yu, Z. and Zhou, X. (2019). "Mechanical behavior of high-strength bolts in T-stubs based on moment distribution", *Engineering Structures*, 196, 109334, <https://doi.org/10.1016/j.engstruct.2019.109334>.
- Berrosipi Aquino, G.J., Gómez Amador, A.M., Alencastre Miranda, J.H. and Jiménez de Cisneros Fonfría, J.J. (2021). "A review of the T-stub components for the analysis of bolted moment joints", *Applied Sciences*, 11(22), 10731, <https://doi.org/10.3390/app112210731>.
- Boudia, S.B.M., Boumechra, N., Bouchair, A. and Missoum, A. (2020). "Modeling of bolted endplate beam-to-column joints with various stiffeners", *Journal of Constructional Steel Research*, 167, 105963, <https://doi.org/10.1016/j.jcsr.2020.105963>.
- Bursi, O.S. and Jaspert, J.P. (1998). "Basic issues in the finite element simulation of extended end plate connections", *Computers and structures*, 69(3), 361-382, [https://doi.org/10.1016/s0045-7949\(98\)00136-9](https://doi.org/10.1016/s0045-7949(98)00136-9).
- Gašić, V., Arsić, A. and Zrnić, N. (2021). "Strength of extended stiffened end-plate bolted joints: Experimental and numerical analysis", *Structures*, 33, 77-89, <https://doi.org/10.1016/j.istruc.2021.04.016>.
- Ghassemieh, M., Mortazavi, S.M.R. and Valadbeigi, A. (2021). "The effect of out of plane perpendicular beams on the ductility demand of steel moment framed structures during progressive collapse", *Civil Engineering Infrastructures Journal*, 54(1), 75-92, <https://doi.org/10.22059/cej.2020.288767.1612>.
- Grogan, W. and Surtees, J.O. (1999). "Experimental behaviour of end plate connections reinforced with bolted backing angles", *Journal of Constructional Steel Research*, 50(1), 71-96, [https://doi.org/10.1016/s0143-974x\(98\)00227-2](https://doi.org/10.1016/s0143-974x(98)00227-2).
- Herath, H.M.H.K., Jayaweeraratne, R.S.S.A. and Wijesundara, K.K. (2023). "Performance-based design method for bolted stiffened end-plate connection under monotonic loading", *Structures*, 53, 214-227, <https://doi.org/10.1016/j.istruc.2023.04.088>.
- Kaushik, K., Sharma, A.K. and Kumar, R. (2013). "A review on finite element analysis of beam to column endplate bolted connection", *IOSR Journal of Mechanical and Civil Engineering*, 8(1), 97-103, <https://doi.org/10.9790/1684-08197103>.
- Kendall, G., Belyi, A. and Elkady, A. (2024). "Experimental investigation of welded steel t-stub components under high loading rates", *Journal of Constructional Steel Research*, 220, 108851, <https://doi.org/10.1016/j.jcsr.2024.108851>.
- Khani, R., Hosseinzadeh, Y., D'Aniello, M. and Hoseinzadeh Asl, M. (2024). "Nonlinear response of coupled and tied-to-rigid base t-stub

- connections", *Journal of Constructional Steel Research*, 215, 108550, <https://doi.org/10.1016/j.jcsr.2024.108550>.
- Krishnamurthy, N. and Graddy, D.E. (1976). "Correlation between 2- and 3-dimensional finite element analysis of steel bolted end-plate connections", *Computers and Structures*, 6(4-5), 381-389, [https://doi.org/10.1016/0045-7949\(76\)90016-x](https://doi.org/10.1016/0045-7949(76)90016-x).
- Labibzadeh, M., Kordi, M., Hosseinlou, F., Rezaeian, A. and Khayat, M. (2025). "Optimizing the performance of L-shaped concrete-filled steel tube columns under eccentric loading", *Civil Engineering Infrastructures Journal*, 58(2), 429-437, <https://doi.org/10.22059/cej.2024.372952.2018>.
- Lin, T., Wang, Z., Hu, F. and Wang, P. (2022). "Finite-element analysis of high-strength steel extended end-plate connections under cyclic loading", *Materials*, 15(8), 2912, <https://doi.org/10.3390/ma15082912>.
- Luo, L., Du, M., Yuan, J., Shi, J., Yu, S. and Zhang, Y. (2020). "Parametric analysis and stiffness investigation of extended end-plate connection", *Materials*, 13(22), 5133, <https://doi.org/10.3390/ma13225133>.
- Luo, L., Shi, J., Qu, Y. and Pan, W. (2023). "Failure evolution analysis of end-plate connection joint based on structural stressing state theory", *Journal of Building Engineering*, 68, 106137, <https://doi.org/10.1016/j.jobe.2023.106137>.
- Lyu, J., Yan, S., He, S., Zhao, X. and Rasmussen, K. (2023). "Mechanical model for the full range behaviour of bolted t-stubs", *Journal of Constructional Steel Research*, 200, 107652, <https://doi.org/10.1016/j.jcsr.2022.107652>.
- Meng, B., Li, F., Zhong, W., Zheng, Y. and Du, Q. (2023). "Strengthening strategies against the progressive collapse of steel frames with extended end-plate connections", *Engineering Structures*, 274, 115154, <https://doi.org/10.1016/j.engstruct.2022.115154>.
- Moore, D.B. and Sims, P.A.C. (1986). "Preliminary investigations into the behaviour of extended end-plate steel connections with backing", *Journal of Constructional Steel*, 6(2), 95-122, [https://doi.org/10.1016/0143-974x\(86\)90001-5](https://doi.org/10.1016/0143-974x(86)90001-5).
- Nawar, M., Elshafy, A., Eltaly, B. and Kandil, K. (2021). "Experimental and numerical analysis of steel beam-column connections", *ERJ. Engineering Research Journal*, 44(1), 43-49, <https://doi.org/10.21608/erjm.2021.36627.1033>.
- Nip, T.F. and Surtees, J.O. (2011). "Threaded bar compression stiffening for moment", *Proceedings of the Second International Conference on Advances in Steel Structures*, Hong Kong, <https://doi.org/10.1016/b978-008043015-7/50034-8>.
- Noferești, H. and Gerami, M. (2023). "Cyclic behavior of bolted stiffened end-plate moment connections for different bolt pretensioning levels: an experimental study", *Shock and Vibration*, 5330905, <https://doi.org/10.1155/2023/5330905>.
- Özkılıç, Y.O. (2023). "Cyclic and monotonic performance of unstiffened extended end-plate connections having thin end-plates and large-bolts", *Engineering Structures*, 281, 115794, <https://doi.org/10.1016/j.engstruct.2023.115794>.
- Özkılıç, Y.O. (2021). "The capacities of thin plated stiffened t-stubs", *Journal of Constructional Steel Research*, 186, 106912, <https://doi.org/10.1016/j.jcsr.2021.106912>.
- Özkılıç, Y.O. and Topkaya, C. (2021). "The plastic and the ultimate resistance of four-bolt extended end-plate connections", *Journal of Constructional Steel Research*, 181, 106614, <https://doi.org/10.1016/j.jcsr.2021.106614>.
- Packer, J.A. and Morris, L.J. (1977). "A limit state design method for the tension region of bolted beam-column connections", *The Structural Engineer*, 55(10), 446-458, [https://www.istructe.org/journal/volumes/volume-55-\(published-in-1977\)/issue-10/a-limit-state-design-method-for-the-tension-region](https://www.istructe.org/journal/volumes/volume-55-(published-in-1977)/issue-10/a-limit-state-design-method-for-the-tension-region).
- Prabha, P., Seetharaman, S., Jayachandran, S.A. and Marimuthu, V. (2011). "Mimicking expensive experiments by Abaqus", *Scientists*, Structural Engineering Research Centre, CSIR Campus, Taramani, Chennai, 600, 113.
- Prinz, G.S., Nussbaumer, A., Borges, L. and Khadka, S. (2014). "Experimental testing and simulation of bolted beam-column connections having thick extended endplates and multiple bolts per row", *Engineering Structures*, 59, 434-447, <https://doi.org/10.1016/j.engstruct.2013.10.042>.
- Sabuwala, T., Linzell, D. and Krauthammer, T. (2005). "Finite element analysis of steel beam to column connections subjected to blast loads", *International Journal of Impact Engineering*, 31(7), 861-876, <https://doi.org/10.1016/j.ijimpeng.2004.04.013>.
- Saravanan, M., Arul Jayachandran, S., Marimuthu, V. and Prabha, P. (2009). "Advanced analysis of cyclic behaviour of plane steel frames with semi-rigid connections", *Steel and Composite Structures*, 9(4), 381-395, <https://doi.org/10.12989/scs.2009.9.4.381>.
- Selamet, S. and Garlock, M. (2010). "Guidelines for modeling three dimensional structural connection models using finite element methods", *In International Symposium: Steel Structures: Culture and Sustainability*. Istanbul, Turkey, <http://ce.boun.edu.tr/selamet/publications/ECCS2010.pdf>.

- Sethi, A. and Warda, B. (2014). "Finite element modeling of t-stub connections reinforced with threaded bars", In *Proceedings of the 2nd European Conference on Earthquake Engineering and Seismology (2nd ECEES)*, Istanbul, Turkey.
- Sethi, A. (1989). "Non-welded reinforcements in bolted steel beam/column connections", PhD Dissertation, University of Leeds, Department of Civil Engineering.
- Shabanzadeh, E., Abdollahzadeh, G.R. and Naghipour, M. (2019). "The Effect of the slot length on beam vertical shear in i-beams with moment connections", *Civil Engineering Infrastructures Journal*, 52(1), 59-84, <https://doi.org/10.22059/ceij.2019.250273.1456>
- Shaheen, M.A. (2022). "A new idea to improve the cyclic performance of end plate beam-column connections", *Engineering Structures*, 253, 113759, <https://doi.org/10.1016/j.engstruct.2021.113759>.
- Sherbourne, A.N. (1961). "Bolted beam-to-column connections", *The Structural Engineer*, 39(6), 203-210, [https://www.istructe.org/journal/volumes/volume-39-\(published-in-1961\)/issue-6/bolted-beam-to-column-connexions](https://www.istructe.org/journal/volumes/volume-39-(published-in-1961)/issue-6/bolted-beam-to-column-connexions).
- Shi, Y., Shi, G. and Wang, Y. (2007). "Experimental and theoretical analysis of the moment-rotation behaviour of stiffened extended end-plate connections", *Journal of Constructional Steel Research*, 63(9), 1279-1293, <https://doi.org/10.1016/j.jcsr.2006.11.008>.
- Tagawa, H. and Gurel, S. (2005). "Application of steel channels as stiffeners in bolted moment connections", *Journal of Constructional Steel Research*, 61(12), 1650-1671, <https://doi.org/10.1016/j.jcsr.2005.04.004>.
- Tagawa, H. and Liu, Y. (2014). "Stiffening of bolted end-plate connections with steel member assemblies", *Journal of Constructional Steel Research*, 103(1), 190-199, <https://doi.org/10.1016/j.jcsr.2014.09.005>.
- Tartaglia, R., D'Aniello, M. and Zimbru, M. (2020). "Experimental and numerical study on the T-stub behaviour with preloaded bolts under large deformations", *Structures*, 27, 2137-2155, <https://doi.org/10.1016/j.istruc.2020.08.039>.
- Wang, P., Pan, J., Wang, Z., Li, B. and Qin, J. (2020). "Experimental and numerical investigation of stiffened angle connection in a minor axis", *Science Progress*, 103(4), 0036850420973521, <https://doi.org/10.1177/0036850420973521>.
- Wang, W., Qian, Z., Zhang, Y. and Wang, Z. (2024a). "Experimental and numerical study on behaviour of extended end-plate connections with Q960 steel at elevated temperature", *Journal of Constructional Steel Research*, 213, 108384, <https://doi.org/10.1016/j.jcsr.2023.108384>.
- Wang, Y., Sun, L., Wang, P., Hou, G., Cai, X. and He, M. (2024b). "Feasibility study of TSOB replacing standard high-strength bolt in T-stub connection", *Structures*, 62, 106246, <https://doi.org/10.1016/j.istruc.2024.106246>.
- Yılmaz, O. and Bekiroğlu, S. (2022). "Biaxial cyclic behavior of bolted end-plate connection to i-column reformed by box-plates", *Engineering Structures*, 255, 113955, <https://doi.org/10.1016/j.engstruct.2022.113955>.
- Zhu, X., Wang, P., Liu, M., Tuoya, W. and Hu, S. (2017). "Behaviors of one-side bolted T-stub through thread holes under tension strengthened with backing plate", *Journal of Constructional Steel Research*, 134, 53-65, <https://doi.org/10.1016/j.jcsr.2017.03.010>.
- Zoetemeijer, P. (1974). "A design method for the tension side of statically loaded, bolted beam-to-column connections", *HERON*, 20(1), 3-59, <https://resolver.tudelft.nl/uuid:f2dff8e5-dd92-4a3c-89db-c4fa945ea759>.

7. Nomenclature

A_s :	Bolt nominal section
d_f :	Distance between the centers of the beam flanges
D_m :	Horizontal displacement
E :	Modulus of elasticity
f_y :	Yield stress
f_u :	Bolt ultimate stress
F_p :	Pre-tension load
S :	Von misses stress
U :	displacement
S :	Von misses stress
α :	Rotation
μ :	Friction coefficient



This article is an open-access article distributed under the terms and conditions of the Creative Commons Attribution (CC-BY) license.